

DOI: 10.1002/adma.200700515

Nanowire-Based High-Performance “Micro Fuel Cells”: One Nanowire, One Fuel Cell**

By Caofeng Pan, Hui Wu, Cheng Wang, Bo Wang, Lu Zhang, Zhida Cheng, Ping Hu,
Wei Pan, Zhaoying Zhou, Xing Yang, and Jing Zhu*

Numerous investigations have resulted in novel nanodevices and applications based on nanomaterials; examples include biosensors,^[1] resonators,^[2] transistors,^[3] in situ real-time biomedical monitoring and detection,^[4] and optoelectronics.^[5] Unfortunately, such devices currently cannot work without an external power supply. A nanometer-sized power source would overcome this problem; development of such a “nano” power source is therefore urgently needed. Among the increasing number of studies on nanodevices, several research groups have reported research into power sources at the nanoscale.^[6–9]

Fuel cells have many advantages over conventional batteries, including more rapid recharging and much higher energy storage density. It is expected that fuel cells of sizes in the nanometer range will be accomplished eventually.

In the current study, we present the first micrometer-sized fuel cell using Nafion/poly(vinyl pyrrolidone) (PVP) nanowires (NPNWs) as the electrolyte. A “micro fuel cell” was monolithically integrated on a silicon substrate and consisted of NPNWs, PtRu/C and Pt/C catalysts, two outleaving electrodes, methanol as fuel, and air as oxidant (see Fig. 1). The performance of the micro fuel cell was orders of magnitude higher than that of a traditional fuel cell power source. The developed micro fuel cell may be integrated

monolithically with other nanodevices rendering such nanodevices self-powered. This approach could provide integrated self-powered nanodevices in the future. Moreover, we researched the proton conductivity (σ_{H^+}) in an individual nanowire with varying nanowire diameter. A strong dependence of the proton conductivity on the diameter in NPNWs was revealed experimentally.

The NPNWs used in this study were synthesized by electrospinning.^[10] The addition of PVP greatly reduces the cost and increases the processability. The PVP serves only as a framework in the NPNWs due to its high molecular weight (1 300 000) and because PVP does not contribute to the proton conductivity. Surface morphology studies performed using scanning electron microscopy (SEM) and energy dispersive X-ray (EDX) analysis of a nanowire showed that the NPNW had a homogeneous diameter (Fig. 2a) and consisted only of the elements C, O, F, and S (Fig. 2b). The length of the prepared nanowires reached up to several millimeters and the diameter range was controllable from about 100 nm up to several micrometers. The near-IR Raman and IR spectra of the Nafion membrane and the prepared nanowires are shown in Figure 2c and d, respectively. The peaks of Nafion were consistent with each other over the whole working wavenumber range.^[11–13] The peaks in the Raman spectrum marked with a triangle refer to PVP (Fig. 2c) and the peak with the black dot at 1252 cm^{-1} was attributed to the silicon substrate. A Raman enhancement appeared at 1053 cm^{-1} , which may have been caused by a surface-enlarged Raman spectroscopy (SERS) effect from the 50 nm gold film (Fig. 2c). Both the Raman and IR spectra demonstrated that the as-synthesized nanowires were indeed composed of Nafion and PVP and that the structure of Nafion was unchanged after the electrospinning process.

After sputtering the silicon dioxide layer, coating the PtRu/C and Pt/C catalysts, and leading out the two electrodes, the performance of the micro fuel cell was tested using a semiconductor characterization system. The fuel was an aqueous solution containing 0.1 M methanol and 1.0 mM H_2SO_4 and the oxidant is ambient air.

The cell voltage and current were measured as a function of the external resistance after the two electrodes were connected externally to a variable resistor. Figure 3 shows the cell potential and the power density (P_n) of the micro fuel cell as a function of the current density (I_d) for temperatures of 298 and 333 K, respectively. The micro fuel cell generated a 314 mV open-circuit voltage (OCV), a maximum I_d of about

[*] Prof. J. Zhu, Dr. C. F. Pan, L. Zhang, Z. D. Cheng
National Center for Electron Microscopy, Laboratory of Advanced
Materials, Department of Material Science and Engineering,
Tsinghua University
Beijing 100080 (P.R. China)
E-mail: jzhu@mail.tsinghua.edu.cn

Prof. W. Pan, Dr. H. Wu
State Key Laboratory of New Ceramic and Fine Processing,
Department of Material Science and Engineering, Tsinghua Uni-
versity
Beijing 100080 (P.R. China)

Prof. C. Wang
Institute of Nuclear and New Energy Technology, Tsinghua
University
Beijing 100080 (P.R. China)

Prof. P. Hu, Dr. B. Wang
Institute of Polymer Science & Engineering, Tsinghua University
Beijing 100080 (P.R. China)

Prof. Z. Y. Zhou, Prof. X. Yang
Department of Precision Instruments & Mechanology, Tsinghua
University
Beijing 100080 (P.R. China)

[**] This work was financially supported by the National 973 Project of
China, the Chinese National Natural Science Foundation, and the
National Centre for Nanoscience and Technology of China.

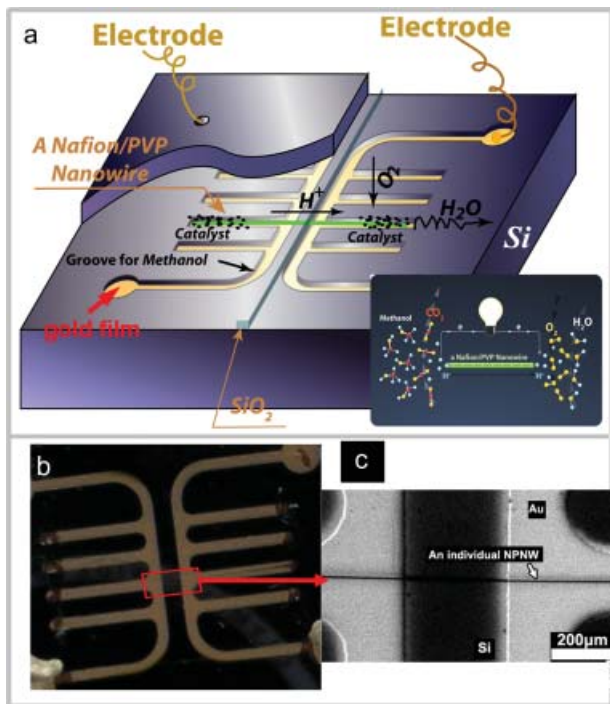


Figure 1. a) Schematic 3D representation of the structure of the micro fuel cell. A groove in the Si substrate (with a 50 nm Au film deposited on the groove) serves simultaneously as a “microchannel” fuel container and an electrode. The NPNWs were kept in place on the Si substrate by mounting a silicon oxide “dam” (of 100 μm width and several μm thickness) on top in the middle of the silicon substrate. The inset shows the working principle of the micro-fuel cell. b) A top-view (overhead view) of the micro fuel cell. c) A magnified image of the area marked by the red rectangle in (b).

1.21 μA/μm² (at zero applied load), and a maximum P_n of about 0.095 μW/μm² at room temperature (shown as the solid curves in Fig. 3a). The OCV is only about half the value of the theoretically generated voltage of the reaction, which can be attributed to the large overpotential required for O₂ reduction and the slow oxidation kinetics of methanol oxidation. From Figure 3a it is clear that the performance of the micro fuel cell improved dramatically with increasing temperature. The performance of the micro fuel cell at 333K (shown as dashed curves in Fig. 3a) reveals an increase of the OCV of over 100 mV. The maximum I_d (at zero applied load) increased by a factor of three and the maximum P_n was 0.348 μW/μm².

The designed micro fuel cell allowed use of different fuels and oxidants. For instance, methanol could be replaced by formic acid as the fuel and pure O₂ could be used as the oxidant instead of air. Figure 3b shows the performance of the micro fuel cell for various combinations of fuel and oxidant. In addition to the methanol/air combination (the dotted curve in Fig. 3a) the performances of fuel cells with combinations of methanol/pure O₂ (dashed curve, Fig. 3b) and formic acid/air (solid curve, Fig. 3b), were also investigated.

Despite the fact that the use of formic acid as fuel has some disadvantages, such as CO poisoning of the Pt catalyst, it is a

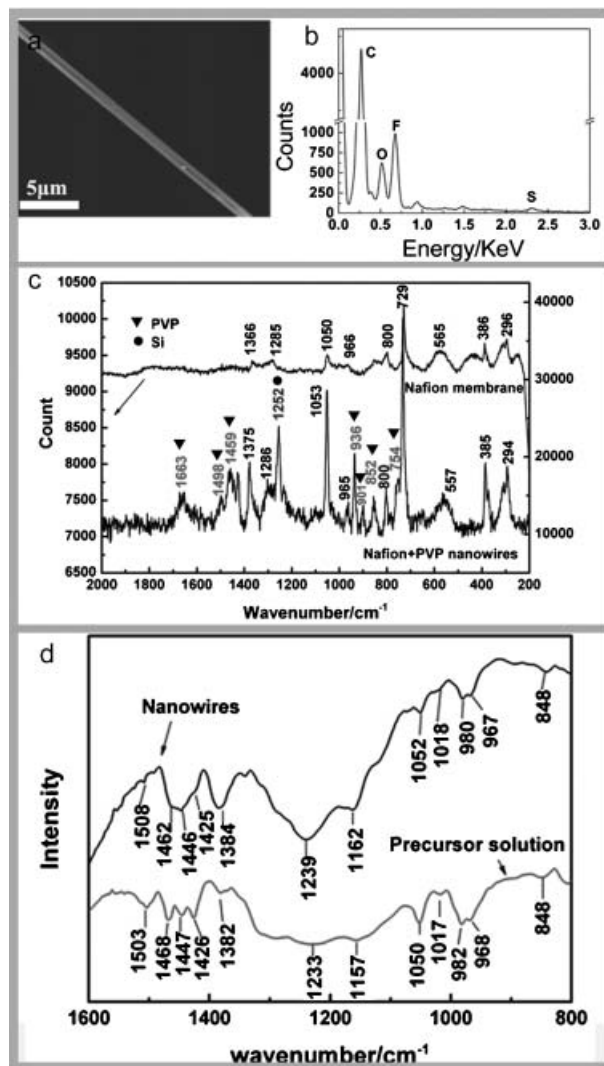


Figure 2. a) An SEM image of the morphology of a single NPNW synthesized by electrospinning shows the NPNW with a homogeneous diameter of about 800 nm. NPNWs with diameters ranging from 100 nm to 16 μm were fabricated successfully. b) EDX spectrum of a NPNW showing that the NPNWs only consisted of the elements C, O, F and S. No contamination was found in the NPNWs. c) Raman spectrum of a NPNW. d) IR spectrum of a NPNW. The spectra shown in (c) and (d) demonstrate that the structure in NPNWs is consistent with that in the Nafion precursor.

convenient and easily controllable fuel, which allowed careful parameter optimization of the initial micro fuel cell design.^[14] The performance of formic acid/air fuel cells at 333 K was lower than that of methanol/air fuel cells at 333 K, (comparable to a methanol/air cell at 318 K).

To determine the influence of the oxygen concentration on the micro fuel cell performance, the oxidant was changed from air (21% oxygen) to pure oxygen. To carry out these experiments, the micro fuel cell was placed in a hermetically-sealed apparatus after the fuel was fed into the microchannel. As might be expected and can be seen from Figure 3b, the

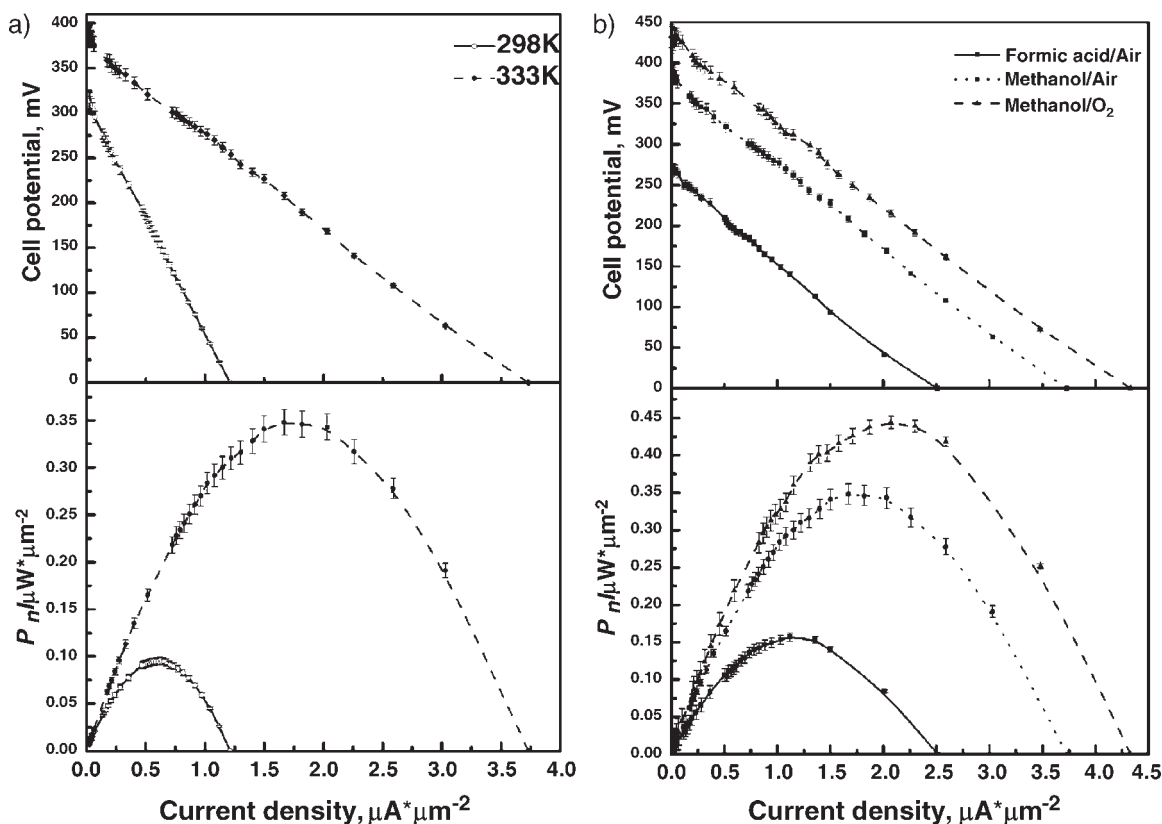


Figure 3. Performance of a micro fuel cell with a single NPNW ($d \approx 2.1 \mu\text{m}$). (a) Current-voltage characteristics (upper graph) and Current-Power Density characteristics (lower graph) measured at two different temperatures. Fuel: 0.1 M methanol/1.0 mM H_2SO_4 ; oxidant: air. (b) Current-voltage characteristics (upper graph) and Current-Power Density characteristics (lower graph) measured at 333 K for various fuel/oxidant combinations. Solid line: fuel /oxidant are formic acid/air, respectively. Dotted line: methanol/air. Dashed line: methanol/oxygen.

performance of the micro fuel cell was enhanced when using pure O_2 as the oxidant. The maximum P_n being generated was about $0.44 \mu\text{W}/\mu\text{m}^2$ and the OCV was over 430 mV at 333 K. It is generally accepted that the kinetic rate of oxygen reduction has a first-order dependence on the oxygen concentration. Consequently, a change of the oxidant from air to oxygen (increasing the oxygen concentration by nearly a factor five) should result in a fivefold increase of the kinetically-controlled oxygen reduction current. The results in Figure 3b show that at high values of cell potential, the cell current at a given potential increased by a factor of five when pure oxygen was used as the oxidant instead of air. However, this factor decreases to less than two with increasing cell current.

We also investigated the dependence of the proton conductivity on the NPNW diameter. Change in the proton conductivity of the NPNWs was experimentally observed when the NPNW diameter was varied over a range of 500 nm to $16.6 \mu\text{m}$ (see Fig. 4a). The measured proton conductivity of the NPNWs started to increase sharply with decreasing NPNW diameter for diameters smaller than $2.5 \mu\text{m}$. The proton conductivity for NPNWs with diameters smaller than $2.5 \mu\text{m}$ was significantly higher than that in the Nafion membrane.^[15] The enhancement of the experimental proton conductivity caused a large increase of the maximum current-density (I_d) of

the micro fuel cell; the measured I_d for the micro fuel cell ($d_{\text{nanowire}} = 2.1 \mu\text{m}$) was $1.21 \mu\text{A}/\mu\text{m}^2$ at 298 K, which is about 10^4 times higher than maximum I_d values reported for traditional fuel cells.^[16] It was interesting to note that double logarithmic plots of the proton conductivity (σ_{H^+}) versus the diameter (d) show a good linear relationships of $\log(\sigma_{\text{H}^+}) = -2.2 \log(d) - 2.74$ within the measured diameter range (500 nm to $16.6 \mu\text{m}$).

As demonstrated by Rubatat et al.,^[17] Nafion shows rodlike or ribbonlike structures in solution. During the preparation of a Nafion membrane, the extrusion of the sulphonyl fluoride precursor may introduce preferential microstructural orientation in the direction of the electrospinning apparatus, which can affect the proton conductance properties of the ionomer.^[18] Therefore, preferential orientation of the rodlike Nafion aggregates may have occurred during the electrospinning process of our experiments. As a result, the longitudinal direction of the rodlike aggregates was thought to be parallel to the longitudinal direction of the NPNWs due to the confinement of the NPNWs' diameter (Fig. 4). The degree of the "texture" resulting from preferential orientation increases with decreasing diameter. Consequently, the transportation of protons in the NPNWs becomes more unblocked, allowing protons to reach the cathode more easily. As a result,

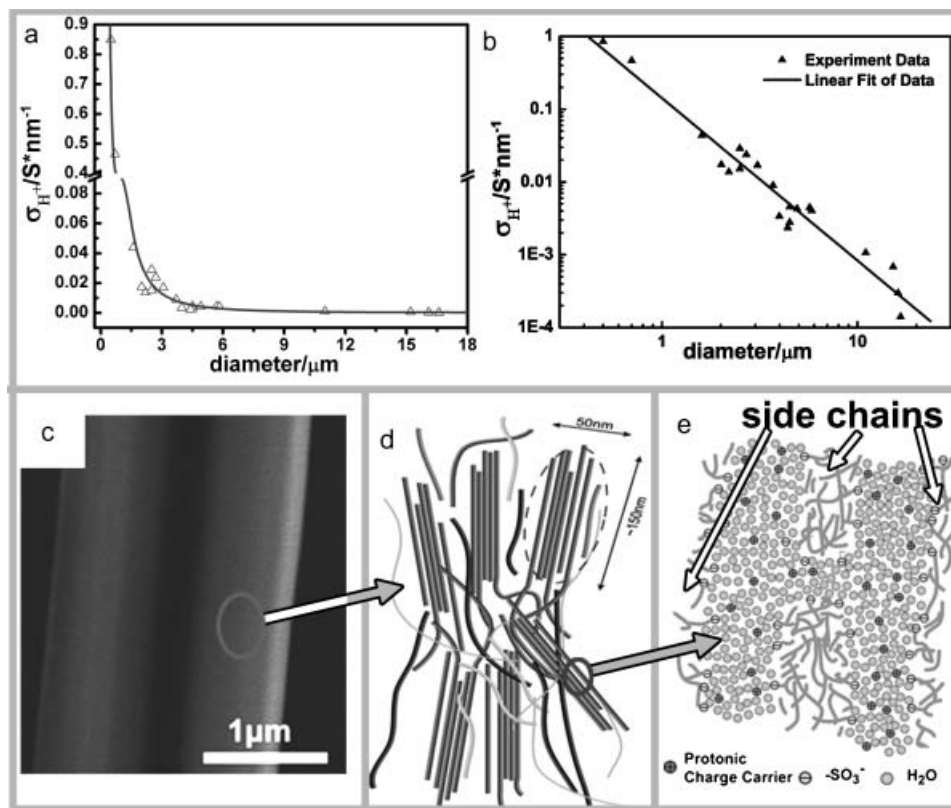


Figure 4. a) Dependence of the proton conductivity (σ_{H^+}) in NPNWs on the diameter (d) of the NPNWs within a diameter range from 500 nm to 16.6 μm . The experimental data (white triangles) were fitted with a power function (black line). b) Double logarithmic plot of the proton conductivity (σ_{H^+}) versus the diameter (d) of the NPNWs. The experimental data (shown as black triangles) show a good linear fit between $\log(\sigma_{H^+})$ and $\log(d)$. c) An SEM image of a single NPNW with a diameter of about 1.91 μm . d) Schematic representation of an entangled network of elongated rodlike aggregates in NPNWs. The aggregates show a tendency for parallel arrangement along the direction of the NPNW. e) Stylized view of the nanoscopic proton transport channel formed by the sulfonic groups in NPNWs, which shows that the proton transport channel parallel to the nanowire is dominant.

the proton conductivity of NPNWs showed a very strong increase with decreasing diameter of the NPNW.

Finally, we made an estimate of the possibility of powering nanodevices and portable electronic devices with a NPNW-based micro fuel cell. The power generated by a single 2.1 μm NPNW-based micro fuel cell was about 1.54 μW , which is enough to drive low-power-consuming complementary metal-oxide semiconductor (CMOS) circuits^[19] and certain nanodevices, for example photosensitive sensors.^[20] However, the power generated by a single NPNW-based micro fuel cell is too small to serve as a power source for portable electronics like a personal digital assistant (PDA) or a laptop, despite the fact that the power density of the presented micro fuel cell is very high. This limitation can be overcome by increasing the number of the nanowires. For example, in a 7 cm \times 0.5 cm \times 0.5 cm volume, 10^5 nanowires with a diameter of 500 nm and a spacing between two nanowires of about 200 nm can be arranged by aligned electrospinning,^[21] after which tens of such devices can be stacked together. The entire assembly of micro fuel cells would occupy a space of 7 cm \times 2 cm \times 2 cm and would generate enough power to serve as a power source for various portable electronic devices, potentially making

micro fuel cells a strong competitor to conventional batteries in the future.

In summary, a novel micro fuel cell has been investigated systematically. The best performance of the developed micro fuel cell was obtained with PtRu/C and Pt/C as catalysts and 0.1 M methanol/1.0 mM H_2SO_4 and pure O_2 as reactants: the open circuit voltage was 0.43 V and the current density and maximum power density were approximately 4.33 $\mu\text{A}/\mu\text{m}^2$ and 0.44 $\mu\text{W}/\mu\text{m}^2$, respectively, at 333 K. These results showed that the performance of the micro fuel cell was several orders of magnitude higher than that of traditional fuel cell power sources. Furthermore, we revealed that the proton conductivity in NPNWs was dependent on the NPNW diameter. The proton conductivity could be enhanced by orders of magnitude when using NPNWs with a diameter of less than 2.3 μm . NPNW-based micro fuel cells may provide a great future for integrated, self-powered nanodevices.

Experimental

Fabrication of Silicon Substrates: The micro fuel cell was monolithically integrated on a silicon substrate. A standard photolithographic

process was used for fabricating the silicon substrates. Subsequently, a gold film of 50 nm thickness deposited by ion sputtering was deposited in the microchannel to serve as an electron collector. Briefly, the silicon wafer was cleaned, dried, and then coated with three layers of photoresist using a spinner. The photoresist was baked at 373 K for 3 minutes. The channel pattern from the photomask was then transferred to the photoresist film using an ABM aligner (ABM, San Jose CA). After the exposed photoresist was dissolved in a developer solution (5 wt% NaOH) for about 2 min, the wafer was rinsed in distilled water; then, the remaining photoresist on the wafer was hard-baked at 373 K for 5 min. After the wafer was cooled, the microchannel was etched by an inductively coupled plasma (ICP) process. The as-prepared microchannel had a width of about 250 μm .

Synthesis of NPNWs Through Electrospinning: Electrospinning provided a simple and versatile method for producing polymer fibers. A precursor polymer solution was prepared containing 1.27 g of 10% Nafion (E. I. DuPont Company, equivalent weight (EW)=1100), 0.26 g of PVP (MW \sim 1 300 000, Sigma) and 2.1 mg of tetramethylammonium chloride (Sigma) in 0.7 g ethanol. In a typical procedure, the precursor polymer solution was loaded into a plastic syringe equipped with a stainless-steel needle made and the distance between the needle tip and the collector was 10 cm. The needle was connected to a high-voltage power supply (operated at 16 kV) during electrospinning, after which the Nafion/PVP solutions were electrospun. The collector used here was composed of two conductive substrates separated by a void gap. Then the as-synthesized NPNWs were transferred onto the as-prepared silicon substrate as shown in Figure 1.

Procedure for Making a Micro Fuel Cell: After transferring the NPNWs onto the silicon substrate, a silicon dioxide layer was sputtered on the Si substrate about halfway of the NPNWs, which served to separate the cathode and the oxide area (see Fig. 1a). PtRu/C and Pt/C catalysts were dispersed into alcohol to give a 2 mg/mL suspension; 0.5 mL of the prepared suspension was coated onto the cathode and the oxide area. After evaporation of the alcohol, the PtRu/C and Pt/C catalysts absorbed onto the NPNWs. After leading out the two electrodes, the micro fuel cell was packaged as shown in Figure 1a.

SEM images and EDX images were obtained using a Hitach 5500 instrument. Raman spectra were recorded with a Renishaw RM2000 microscopic confocal Raman spectrometer (operated at 633 nm). The illumination power used was about 4.7 mW. IR absorption spectra were recorded using a Perkin-Elmer GXFTIR system with an accessory for

attenuated total reflection (ATR). The performance of the micro fuel cell was tested on a Keithley 4200SCS semiconductor characterization system.

Received: March 1, 2007

Revised: August 29, 2007

Published online: April 11, 2008

- [1] G. F. Zheng, F. Patolsky, Y. Cui, W. U. Wang, C. M. Lieber, *Nat. Biotechnol.* **2005**, *23*, 1294.
- [2] X. D. Bai, P. X. Gao, Z. L. Wang, E. G. Wang, *Appl. Phys. Lett.* **2003**, *82*, 4806.
- [3] G. F. Zheng, W. Lu, S. Jin, C. M. Lieber, *Adv. Mater.* **2004**, *16*, 1890.
- [4] S. Gross, A. Gilead, A. Scherz, M. Neeman, Y. Salomon, *Nat. Med.* **2003**, *9*, 1327.
- [5] X. F. Duan, Y. Huang, R. Agarwal, C. M. Lieber, *Nature* **2003**, *421*, 241.
- [6] Z. L. Wang, J. H. Song, *Science* **2006**, *312*, 242.
- [7] J. H. Song, J. Zhou, Z. L. Wang, *Nano Lett.* **2006**, *6*, 1656.
- [8] J. V. Hernandez, E. R. Kay, D. A. Leigh, *Science* **2004**, *306*, 1532.
- [9] S. P. Fletcher, F. Dumur, M. M. Pollard, B. L. Feringa, *Science* **2005**, *310*, 80.
- [10] D. Li, Y. L. Wang, Y. N. Xia, *Nano Lett.* **2003**, *3*, 1167.
- [11] A. Gruger, A. Regis, T. Schmatko, P. Colomban, *Vib. Spectrosc.* **2001**, *26*, 215.
- [12] L. Zhang, C. F. Pan, J. Zhu, C. Wang, *Nanotechnology* **2005**, *16*, 2242.
- [13] C. Pan, L. Zhang, J. Zhu, J. Luo, Z. Cheng, C. Wang, *Nanotechnology* **2007**, *18*, 015302.
- [14] E. R. Choban, L. J. Markoski, A. Wieckowski, P. J. A. Kenis, *J. Power Sources* **2004**, *128*, 54.
- [15] G. Alberti, M. Casciola, *Solid State Ionics* **2001**, *145*, 3.
- [16] S. Ha, B. Adams, R. I. Masel, *J. Power Sources* **2004**, *128*, 119.
- [17] L. Rubatat, A. L. Rollet, G. Gebel, O. Diat, *Macromolecules* **2002**, *35*, 4050.
- [18] K. A. Mauritz, R. B. Moore, *Chem. Rev.* **2004**, *104*, 4535.
- [19] R. R. Harrison, C. Koch, *Anal. Integr. Circ. S.* **2000**, *24*, 213.
- [20] The photosensitive sensor was supplied by Prof. Zhaoying Zhou, Tsinghua University.
- [21] D. Li, Y. L. Wang, Y. N. Xia, *Adv. Mater.* **2004**, *16*, 361.